

Epidermal expression of an Elovl4 transgene rescues neonatal lethality of homozygous Stargardt disease-3 mice

Anne McMahon,¹ Igor A. Butovich, and Wojciech Kedziński

Department of Ophthalmology, University of Texas Southwestern Medical Center, Dallas, TX 75390

Abstract Elongase of very long chain fatty acids-4 (ELOVL4) is the only mammalian enzyme known to synthesize C28-C36 fatty acids. In humans, ELOVL4 mutations cause Stargardt disease-3 (STGD3), a juvenile dominant macular degeneration. Heterozygous Stgd3 mice that carry a pathogenic mutation in the mouse Elovl4 gene demonstrate reduced levels of retinal C28-C36 acyl phosphatidylcholines (PC) and epidermal C28-C36 acylceramides. Homozygous Stgd3 mice die shortly after birth with signs of disrupted skin barrier function. In this study, we report generation of transgenic (Tg) mice with targeted Elovl4 expression driven by an epidermal-specific involucrin promoter. In homozygous Stgd3 mice, this transgene reinstates both epidermal Elovl4 expression and synthesis of two missing epidermal lipid groups: C28-C36 acylceramides and (*O*-linoleoyl)-omega-hydroxy C28-C36 fatty acids. Transgene expression also restores skin barrier function and rescues the neonatal lethality of homozygous Stgd3 mice. These studies establish the critical requirement for epidermal C28-C36 fatty acid synthesis for animal viability. In addition to the skin, Elovl4 is also expressed in other tissues, including the retina, brain, and testes. Thus, these mice will facilitate future studies to define the roles of C28-C36 fatty acids in the Elovl4-expressing tissues.—McMahon, A., Igor A. Butovich, and Wojciech Kedziński. Epidermal expression of an Elovl4 transgene rescues neonatal lethality of homozygous Stargardt disease-3 mice. *J. Lipid Res.* 2011. 52: 1128–1138.

Supplementary key words elongase of very long chain fatty acids-4 • very long chain C28-C36 fatty acids • acylceramides • skin permeability barrier

Stargardt disease-3 (STGD3) is a juvenile dominant macular dystrophy caused by mutations in the gene coding for elongase of very long chain fatty acids-4 (ELOVL4)

This work was supported by National Institutes of Health Grants RO1 EY-018395 (W.K.), RO1 EY-01019480 (I.A.B.), and EY-020799 (core grant); and by an unrestricted grant to the Department of Ophthalmology from Research to Prevent Blindness (New York, NY). Its contents are solely the responsibility of the authors and do not necessarily represent the official views of the National Institutes of Health or other granting agencies.

Manuscript received 28 January 2011 and in revised form 21 March 2011.

Published, JLR Papers in Press, March 22, 2011

DOI 10.1194/jlr.M014415

(1–4). All three identified pathogenic mutations lead to synthesis of a truncated ELOVL4 protein deprived of its C-terminal sequence. The deleted sequence contains a peptide motif for retention in the endoplasmic reticulum (1, 2), a site of long chain fatty acid synthesis (5). The truncated protein expressed in cultured cells has been shown to leave the endoplasmic reticulum (6, 7) and to carry associated with it wild-type (wt) ELOVL4 protein (8–10). All these findings suggest that the ELOVL4 pathogenic mutations decrease the efficacy of fatty acid chain elongation, the reaction known to be a rate-limiting step in fatty acid synthesis (11).

ELOVL4 appears to be the only elongase capable of synthesis of fatty acids containing more than 26 carbon atoms. First, such fatty acids have been shown to be synthesized in cultured cells that have been transfected with an ELOVL4 transgene (12). Second, the retinas of heterozygous Stgd3 mice, which carry a human pathogenic 5-bp deletion in the mouse Elovl4 gene, have a deficiency of phosphatidylcholine (PC) lipids that contain acyl residues of polyunsaturated C28-C36 fatty acids (13). This early, selective lipid change is later followed by reduced vision and increased retinal accumulation of toxic lipofuscin products (14). All these findings have suggested that polyunsaturated C28-C36 fatty acids play vital, yet to be determined roles in retinal physiology (15).

To fully comprehend the functions of C28-C36 fatty acids in the retina, and potentially in other Elovl4-expressing tissues, such as skin, brain, lens and testis (1, 16), heterozygous Stgd3 mice were bred to homozygosity. The aim was to generate mature homozygous Stgd3 mice that completely lacked C28-C36 fatty acid synthesis. At birth, retinal development in wt mice is incomplete, and fully functional retinas are not present until mice are about three weeks old. The generated homozygous Stgd3 mice were born at

Abbreviations: ELOVL4, elongase of very long chain fatty acids-4; MS, mass spectrometry; N, nucleotide; PC, phosphatidylcholine; STGD3, Stargardt disease-3; Tg, transgenic; wt, wild-type.

¹To whom correspondence should be addressed.

e-mail: Anne.Mcmahon@utsouthwestern.edu

the expected Mendelian frequency, but they died a few hours after birth showing symptoms of defective skin barrier function (14). This same phenotype has also been reported for all homozygous Elov14-mutant mice that have been generated to date (17–19). Analysis of epidermal lipids in all these mouse mutants revealed a complete absence of acylceramides, which contain residues of saturated and monounsaturated C28-C36 fatty acids.

All these findings suggested a need for generation of viable mature mice that would completely lack C28-C36 fatty acid synthesis in the retina and in other Elov14-expressing tissues. In this article, we describe generation of homozygous Stgd3 mutant mice that express an involucrin promoter-driven Elov14 transgene. With these mice, we sought to answer the following questions: *a*) can epidermal C28-C36 acyl lipid synthesis be restored in homozygous Stgd3 mice by expression of transgenic (Tg) Elov14 in the epidermis, *b*) can expression of the transgene repair the defective skin permeability barrier function in homozygous Stgd3 mice, and *c*) is the defective skin barrier function in homozygous Stgd3 mice the only cause of their neonatal lethality? The results of our studies in the Tg/homozygous Stgd3 mice yield positive answers to all these questions, verifying the importance of Elov14 lipid products for the skin function and animal viability.

MATERIALS AND METHODS

Transgene construction

Total RNA was isolated from retinas of 129SvEv mice (Taconic, Hudson, NY) using RNA-Stat60 reagent following the manufacturer's protocol (Tel-Test, Inc., Friendswood, TX). Then the RNA sample was RT-PCR transcribed using the Superscript III First-Strand cDNA Synthesis System (Invitrogen Corporation, Carlsbad, CA), the High Fidelity PCR System (Stratagene, La Jolla, CA), and Elov14 amplification primers, forward 5'-GCGGC-CGCTGCTCGTACCTCTCCTC and reverse 5'-GCGGCCGACT-GTCTACCGTTAAGGCCAGT. Both primers were designed to incorporate a NotI restriction site on flanking ends of the Elov14 sequence. The amplified DNA was cloned into the pCR-XL-TOPO vector (Invitrogen), verified by sequencing, and released by NotI digestion. The isolated Elov14 DNA fragment was cloned into a NotI-digested pH3700-pL2 plasmid, replacing its NotI-flanked galactosidase insert (20). The pH3700-pL2 plasmid contains a human involucrin promoter, which has been shown to direct specific expression of cloned Tg sequences to stratified squamous epithelia that are present in the epidermis of skin and a few other internal organs, such as the esophagus, forestomach, and tongue (20). The final Elov14 Tg construct was verified by sequencing and digested with SalI to release a 5.1-kb Tg sequence (Fig. 1A).

Generation of transgenic mice

The released 5.1-kb Tg sequence was gel-purified and injected into fertilized oocytes from C57Bl/6 mice in the Transgenic Technology Center, University of Texas Southwestern Medical Center. Derived mice were screened by PCR analysis of tail DNA, and three identified founders were bred with 129SvEv mice. Obtained progeny were then crossed with heterozygous Stgd3 mice, which were on the 129SvEv background (14), to obtain both Tg/heterozygous and Tg/homozygous Stgd3 progeny. Subsequently two of these Tg lines (lines A and C) were bred together to gener-

ate compound Tg^{A+C} mice on the homozygous Stgd3 background. Mice were housed in the University Animal Resource Center under a 12 h light/12 h dark cycle. Retinal samples were collected from mice euthanized in the middle of the daylight cycle.

All experiments with animals were conducted in conformity with the Public Health Service Policy on Human Care and Use of Laboratory Animals, and they were approved by the Institutional Animal Care and Use Committee of the University of Texas Southwestern Medical Center.

Mouse genotyping

Genotyping was performed by PCR analysis of tail DNA using forward 5'-CACTAGAATGCCCTTGCTGAGC and reverse 5'-GGC-TCATTGTATGTCCGAGTGTAGAAGTTG primers for the wt Elov14 allele, and forward 5'-GCCTTGGGGAAACCACAGTAGA and reverse 5'-GCTCTTTGTATGTCCGAGTGTAGGAGGA primers for the Stgd3 (Elov14 mutant) allele. The PCR reaction for the Elov14 transgene used forward 5'-GACCCGGTGTGACTTCCTT-GATC and reverse 5'-TTCCCATAGAACAGGGACTGTGCCAT primers, both containing human involucrin promoter sequence present in the transgene. PCR reactions generated sequence-specific products of 332, 441 and 204 bps for the wt Elov14 allele, Stgd3 allele and Elov14 transgene, respectively (Fig. 1B).

Nuclease protection assay

Total RNA was isolated from mouse dorsal skin (ca. 50 mg) or an eyecup using RNA-Stat60 reagent. Isolated RNA samples were hybridized for 16 h at 68°C with [³²P]labeled riboprobe in a 25 µl mixture containing 40 mM Tris-HCl, pH 7.5, 0.6 M NaCl, 4 mM EDTA, pH 7.5, 4 mM dithiothreitol and 40% formamide. Following hybridization, the samples were digested for 45 min at 50°C with 240 units of S1 nuclease (Invitrogen) added in 150 µl buffer containing 50 mM sodium acetate, pH 4.8, 0.2 M NaCl and 15 mM zinc chloride. After digestion, the samples were extracted with a 0.2 ml phenol/chloroform mixture (1:1, vol:vol), precipitated with ethanol, then dissolved and denatured in 10 µl 80% formamide at 95°C for 2 min, and loaded onto an 8% polyacrylamide gel (0.1 mm Criterion Cassette, Bio-Rad Laboratories, Hercules, CA) containing 6 M urea. After 1.5 h electrophoresis at 120 Volts the gels were analyzed for radioactive riboprobe fragments using a Typhoon 9410 phosphorimager (Amersham Biosciences Corporation, Piscataway, NJ).

Two riboprobes of different lengths were used to analyze mRNA expression. The first, a 320-nucleotide (N) riboprobe (Fig. 1C) which contained (a) 72 Ns complementary to an SV40 polyA sequence present only in Tg mRNA, (b) 177 Ns complementary to an Elov14 sequence present in wt Elov14, Stgd3 and Tg mRNAs, and (c) 71 Ns of the vector sequence. In the assay, both wt Elov14 and Stgd3 mRNAs protected the 177-N Elov14 fragment of the riboprobe. In contrast, Tg mRNA protected this same fragment plus the adjoining 72 Ns SV40 sequence yielding a 249-N protected fragment [Fig. 1D(i) and (ii)].

The second probe, a 414-N riboprobe was used in an assay to examine tissue specific expression of the Elov14 transgene. This probe consisted of three components: (a) a 55-N sequence complementary to a 3'-non-coding Elov14 mRNA fragment present in both wt Elov14 and Stgd3 mRNAs but not in the Tg mRNA, (b) a 287-N sequence complementary to a 3'-coding Elov14 mRNA fragment present in its entirety in wt and Tg mRNAs but only partly in Stgd3 mRNA, and (c) a 72-N vector sequence. In the assay, wt mRNA and Tg mRNA protected 342-N and 287-N riboprobe fragments, respectively (Fig. 9). Protection by the Stgd3 mRNA yielded two riboprobe fragments of 230 and 107 Ns as a consequence of the internal Stargardt-3 pathogenic deletion of five base pairs in the Stgd3 (mutated Elov14) gene.

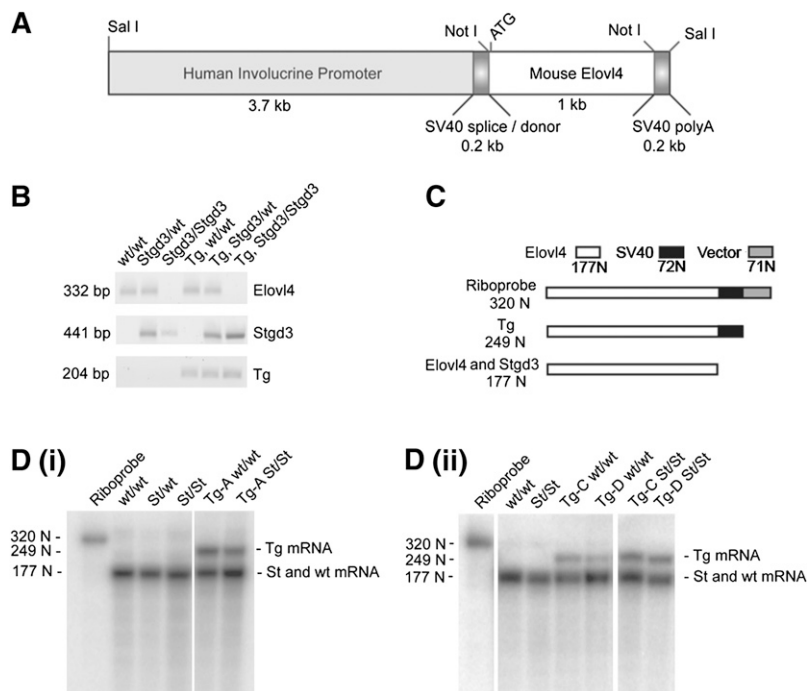


Fig. 1. Generation of Elov4 transgenic mice. A: Construct used to generate Tg mice. The mouse Elov4 coding sequence, preceded by 20 bps of 5'-untranslated sequence, was cloned downstream of the human involucrine promoter sequence and followed by SV40 splice/donor and SV40 polyA tail-addition sequences. The size of each component is shown below the construct schematic. B: Genotyping of mice by PCR analysis of tail DNA samples. The wt Elov4 and Stgd3 alleles and the Elov4 transgene yield specific PCR products of 332, 441, and 204 bps, respectively. The assay allows identification of mice carrying the transgene on wt Elov4 (wt/wt), heterozygous (Stgd3/wt) or homozygous Stgd3 (Stgd3/Stgd3) backgrounds. C: Schematic of the nuclease protection assay designed for analysis of Tg mRNA expression in the skin of neonatal Tg mice. Both the probe and predicted protected fragments are shown. The assay detected Tg mRNA in all three Tg mouse lines as indicated by the presence of a protected 249-N riboprobe fragment [D(i): Tg line A; D(ii): Tg lines C and D].

Thin-layer chromatography of epidermal lipids

Excised dorsal skin of neonatal mice was separated into epidermal and dermal fractions. The epidermal samples were then homogenized in a chloroform/methanol mixture using a glass homogenizer to obtain extractable lipids as we have previously described in detail (14). Lipid extracts were stored under argon at -20°C until analyzed. Thin-layer chromatography of lipids was performed using silica gel 60Å flexible aluminum plates (Whatman, Inc., Piscataway, NJ). The plates were prewashed with a chloroform/methanol mixture, (9:1, vol:vol), air dried, and baked at 120°C for 15 min. Extracted epidermal lipids were resolved by developing twice in a chloroform/methanol/acetic acid mixture (190:9:1, vol:vol:vol) and visualized by spraying with an 8% H_3PO_4 solution containing 10% CuSO_4 , with subsequent charring at 120°C for 15 min (21). Lipid class identification was assigned by comparison to commercial lipid standards and/or by mass spectrometric (MS) analysis. Standards used were cholesterol, cholesterol behenate as a cholesterol ester (Nu-Chek Prep, Inc., Elysian, MN), and N-lignoceroyl-D-erythro-sphingosine [Cer (C24)] as a ceramide standard (Avanti Polar Lipids, Inc., Alabaster, AL). Quantitative evaluation of the relative levels of lipid classes was performed using scanning densitometric analysis (Image Quant) of charred plates using a Typhoon 9410 phosphorimager (Amersham Biosciences Corporation). Signals for acylceramides and X lipids were normalized independently to signals for lipids with Rf values similar to the cholesterol and Cer (C24) standards. The group of lipid species designated as X, which was present in the epidermis of wt but absent in homozygous Stgd3 mice (Fig. 2), had to be identified by MS fragmentation analysis since no standard lipids were available.

Mass spectrometric analysis of epidermal lipids

MS analysis was used to identify two lipid bands designated as AC and X. They were present in wt but absent in homozygous Stgd3 epidermal lipid extracts when analyzed by thin-layer chromatography (Fig. 2). The lipid group in the AC band was extracted from the plate and shown by atmospheric pressure chemical ionization MS analysis in the negative ion mode to have identical m/z values to the acylceramide lipids we previously de-

scribed to be present in neonatal mouse epidermis (14). The lipids in the band designated as X were also analyzed by MS to obtain m/z values for its lipid ions. The obtained m/z data served for reverse phase HPLC/MS and MS collision-induced fragmentation analyses of the lipids of both the band X and total epidermal extracts. The conditions used in HPLC/MS and MS collision-induced fragmentation analysis, and assignment of chemical formulas for analyzed lipids have been described previously (22).

Skin permeability barrier assays

Both toluidine blue and Lucifer yellow dye assays were used to assess skin permeability barrier function in neonatal mice. The toluidine blue penetration assay was performed as previously de-

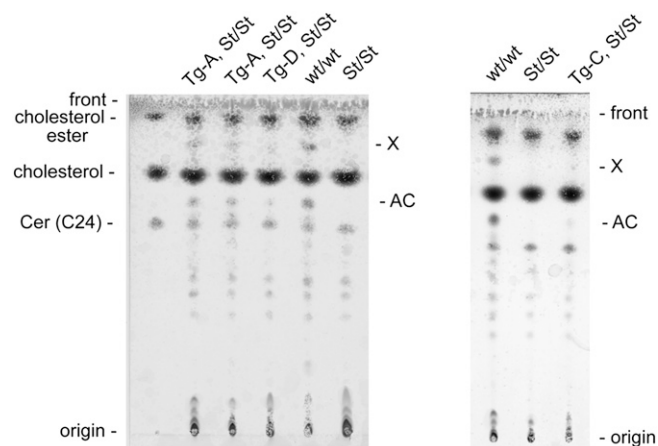


Fig. 2. Thin-layer chromatography analysis of epidermal lipids from neonatal mice. This lipid analysis shows the presence of acylceramides (AC) and (*O*-linoleoyl)- ω -hydroxy C28-C36 fatty acids (X) in neonatal wt Elov4 mice (wt/wt) and their absence in homozygous Stgd3 littermates (St/St). Both lipid groups are restored by Elov4 transgene expression in neonatal Tg/homozygous Stgd3 mice from all three Tg lines (A, Tg lines A and D; B, Tg line C).

scribed (14). For the Lucifer yellow assay, neonatal mice within 1 h of birth were euthanized with sodium pentobarbital (Euthasol, Virbac AH, Fort Worth, TX) and immersed for 1 h at 25°C in 1 mM Lucifer yellow dye (Sigma-Aldrich) dissolved in phosphate buffered saline (PBS). Back skin strips were collected and frozen in Tissue-Tek O.C.T. Compound. Tissues were sectioned at 20 μ m, post fixed for 30 min in 4% paraformaldehyde in PBS (23, 24), washed with PBS, and then nuclei counterstained using TO-PRO-3 dye (Invitrogen). Sections mounted in Gel Mount (Bio-media, Foster City, CA) were imaged on an SP2 laser scanning confocal microscope (Leica Microsystems, Heidelberg, Germany) using a 63 \times water objective. Fluorescent imaging with Ar/ArKr (488 nm) and HeNe (633 nm) lasers was used for excitation of the Lucifer yellow dye and the TO-PRO-3, respectively. Emission collection wavelengths, gain, and offset were optimized for the wt/wt epidermal staining. These values were then used for imaging sections from all mutant mice analyzed. Images obtained from all mouse genotypes were assembled in a single document and processed using Photoshop (Adobe, San Jose, CA).

Analysis of skin morphology

Neonatal mice were euthanized with sodium pentobarbital within 1 h of birth, and their back skin was excised and fixed in 0.1 M cacodylate buffer containing 2% paraformaldehyde and 2% glutaraldehyde. Further processing was performed in the University Electron Microscopy Core Facility using previously described procedures (25). One- μ m skin sections were stained with toluidine blue for light microscopy. Seventy-nm sections were imaged using a FEI Tecnai G2 Spirit Biotwin electron microscope operated at 120 kV. Digital images were captured with a SIS Morada 11 mpixel side mount CCD.

RESULTS

Generation of mice that express an Elov14 transgene in the skin

An Elov14 transgene was constructed to selectively target expression of mouse wt Elov14 to the epidermis of Tg mice using a human involucrin promoter sequence (Fig. 1). The involucrin sequence used has previously been shown to direct specific expression of cloned Tg sequences to stratified squamous epithelia, which are present in the epidermal layer of the skin and in a few internal organs, such as the esophagus, forestomach, and tongue (20). The resulting Elov14 Tg construct was used to generate three Tg founder mice, which were identified by PCR analysis of tail DNA samples (Fig. 1B presents representative results for all possible genotypes). After breeding with wt mice, all founders transferred the transgene to their progeny. No phenotypic changes were observed in any of the mice obtained from these breedings, suggesting an absence of insertional activation or inactivation events as a consequence of the presence of the transgene. Each of the three Tg lines (A, C, and D), originally established on the wt Elov14 background, was subsequently bred onto heterozygous and homozygous Stgd3 backgrounds.

The generated Tg mice from all three Tg lines expressed Tg mRNA in neonatal skin, in addition to endogenous wt Elov14 and/or Stgd3 mRNAs [Fig. 1D(i) and (ii)]. Tg mRNA was expressed at 0.1-0.3 times the level of endogenous Elov14 mRNA, being present at the lowest level in

mice from Tg line D [Fig. 1D(ii)] and at the highest level in mice from line A [Fig. 1D(i)].

Transgene expression restores synthesis of epidermal C28-C36 fatty acids in homozygous Stgd3 mice

Lipids extracted from the epidermis of neonatal mice were analyzed by thin-layer chromatography (Fig. 2). Two major lipid groups, designated as AC and X, were detected in extracts from the wt epidermis but were missing from those isolated from the epidermis of homozygous Stgd3 mice. The presence of both missing lipid groups was restored to the epidermis of homozygous Stgd3 mice by expression of the Elov14 transgene in the skin. Though the amounts of both AC and X lipids detected in the epidermis of the different Tg lines varied, in all cases, the restored levels were lower than the levels present in wt mice. By densitometric analysis of the chromatograms, we estimated that both restored lipid groups were present at approximately 0.1-0.3 times the levels of these lipids in the wt mouse epidermis.

On the basis of available knowledge about Elov14 lipid products, we expected that the two lipid groups, both missing in homozygous Stgd3 mice and restored by Tg Elov14 expression, would contain residues of C28-C36 fatty acids. This prediction was confirmed by HPLC/MS analysis. MS analysis of lipids extracted from the region of the TLC plate designated as AC identified these lipids as acylceramides. These abundant epidermal lipids containing residues of saturated and monounsaturated C28-C36 fatty acids have previously been shown to be depleted from the epidermis of both neonatal homozygous Stgd3 (14) and other Elov14-mutant mice (17-19).

Negative mode MS analyses of the lipids extracted from the area of the TLC plate containing the X lipid group identified two major compounds of m/z 757.8 and 783.5. To confirm these data, total lipid extracts from mouse epidermis were analyzed using reverse phase HPLC/MS. Both peaks of m/z 757.8 and 783.5 were present in the epidermal extracts from neonatal wt mice but were missing in the extracts from homozygous Stgd3 mice (Fig. 3). MS collision-induced fragmentation analysis of the m/z 757.8 lipid detected m/z 279.5 and 495.7 peaks, corresponding to the ions of linoleic acid (m/z 279.1) and hydroxy C32 fatty acid (m/z 495.5), respectively (Fig. 4A). Similar analysis of the m/z 783.5 lipid detected m/z 279.3 and 521.8 peaks corresponding to the ions of linoleic acid (m/z 279.1) and hydroxy C34 fatty acid (m/z 521.5), respectively (Fig. 4B). On the basis of these results and previous MS fragmentation analysis of similar (*O*-linoleoyl)-omega-hydroxy fatty acids of human meibum (22), the chemical structures of m/z 757.8 and 783.5 lipids were proposed to be (*O*-linoleoyl)-omega-hydroxy C32 and (*O*-linoleoyl)-omega-hydroxy C34 fatty acids, respectively (Fig. 4C).

In conclusion, thin-layer chromatography and HPLC/MS analyses have shown that the involucrin-driven Elov14 transgene expression restores epidermal synthesis of C28-C36 fatty acids and their compound lipids, acylceramides and (*O*-linoleoyl)-omega-hydroxy C28-C36 fatty acids, in homozygous Stgd3 mice. The largest amounts of these

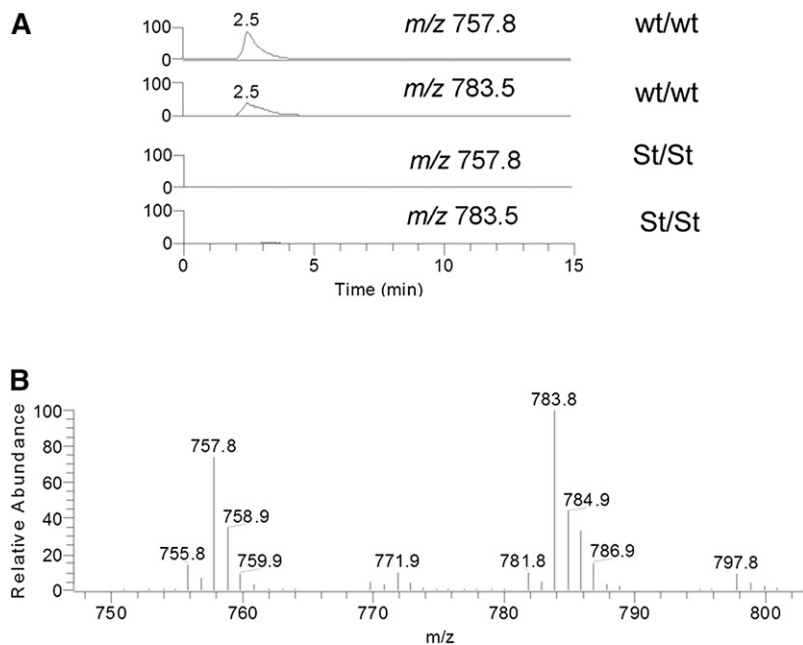


Fig. 3. MS analysis of epidermal X lipids in negative ion mode. Reverse phase HPLC/MS analysis of epidermal lipids detects two ions with m/z 757.8 and 783.5, which are present in wt Elov14 mice (wt/wt) but missing from homozygous Stgd3 mice (St/St). A: Selected ion monitoring (SIM) chromatogram extracted from a total ion chromatogram of epidermal lipids shows the presence of m/z 757.8 and 783.5 peaks in the wt mice and their absence in the homozygous Stgd3 mice. B: Averaged mass spectrum of the HPLC peak with retention time 2.5 min shown in panel A.

lipids were present in Tg lines A and C, which have also been found to contain the highest levels of Tg mRNA in the skin. Both these Tg lines were selected for further studies.

Transgene expression corrects a defective functioning of the skin permeability barrier in homozygous Stgd3 mice

Previously, using a toluidine blue penetration assay, we have demonstrated a defective skin permeability barrier in

neonatal homozygous Stgd3 mice (14). The skin of such mice, but not wt mice, stained blue when immersed in a toluidine blue solution. The current studies showed that this water-soluble dye was also excluded from the skin of Tg/homozygous Stgd3 mice (**Fig. 5**). These findings suggested that epidermal expression of the Elov14 transgene was able to restore the skin permeability barrier in homozygous Stgd3 mice.

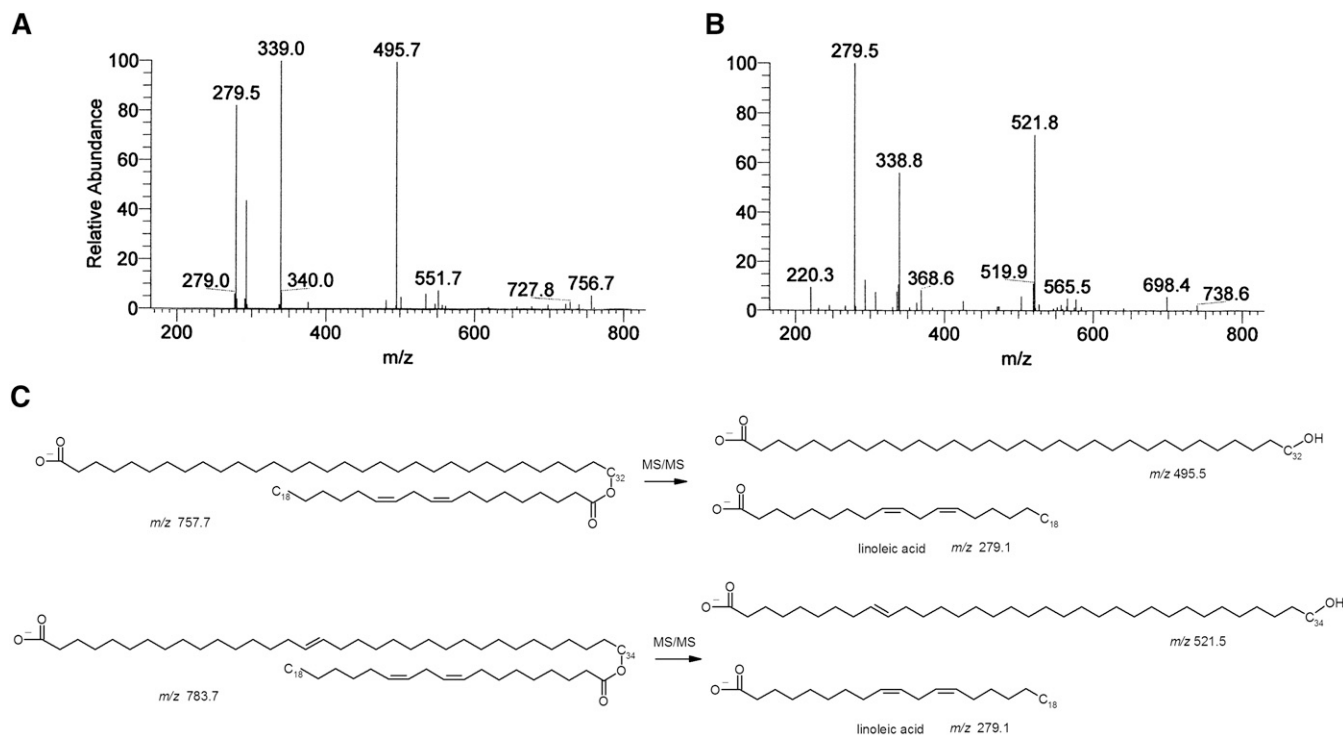


Fig. 4. Structural analysis of X lipid species. MS collision-induced ion spectrum generated from the X lipids, (A) 757.8 and (B) 783.5 m/z species, in the negative ion mode. C: The proposed chemical structures of the X lipids with m/z 757.8 and 783.5, as derived from analysis of the MS collision-induced fragmentation results, are $(O\text{-linoleoyl})\text{-}\omega\text{-hydroxy C}_{32}$ and $(O\text{-linoleoyl})\text{-}\omega\text{-hydroxy C}_{34}$ fatty acids, respectively. The exact location and *cis, trans* geometry of the double bonds in the $(O\text{-acyl})\text{-}\omega\text{-hydroxy-fatty acids}$ have not been determined.

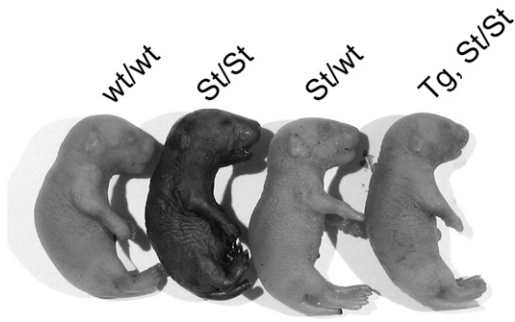


Fig. 5. Epidermal expression of the *Elovl4* transgene restores skin permeability barrier function in homozygous *Stgd3* mice. Toluidine blue penetrated and stained the skin of euthanized neonatal homozygous *Stgd3* mice (*St/St*), but not wt *Elovl4* (*wt/wt*), heterozygous *Stgd3* (*St/wt*), or Tg/homozygous *Stgd3* (*Tg St/St*) mice (*Tg^A* mouse shown).

As a more sensitive assay for barrier function, we also examined epidermal penetration of Lucifer yellow, a fluorescent dye which can subsequently be covalently linked to surrounding biomolecules during aldehyde fixation of tissue (23, 24). In wt mice (**Fig. 6A**), only punctuate staining of the stratum corneum outer surface was observed. In contrast, in homozygous *Stgd3* mice (**Fig. 6B**), the Lucifer yellow dye penetrated the full extent of the stratum corneum, with some penetration also seen into interior epidermal strata. In both lines of Tg/homozygous *Stgd3* mice, the strongest dye staining was detected on the outer surface of the stratum corneum (**Fig. 6C–E**). Weaker staining, to different degrees in both Tg lines, was also seen in interior parts of the stratum corneum. In Tg line C, some skin areas also showed deeper dye penetration to other epidermal strata, (compare **Fig. 6C** and **D**). Staining in *Tg^C* mice on the wt *Elovl4* background (**Fig. 6F**), however, was similar to that observed for wt epidermis. This suggests no adverse consequence of transgene expression on epidermal barrier function. These findings confirmed the previous results of the toluidine blue penetration assay that *Elovl4* transgene expression restores, although not completely, the epidermal permeability barrier in both Tg/homozygous *Stgd3* mouse lines.

Transgene expression corrects pathological changes in skin morphology of homozygous *Stgd3* mice

Light microscopic analysis of skin fixed with 2% paraformaldehyde and 2% glutaraldehyde showed a loose basket weave-like structure of the stratum corneum in wt mice (**Fig. 7A**). On the contrary, in homozygous *Stgd3* mice, the stratum corneum was compact with compressed corneocyte leaflets. Epidermal morphology in the Tg/homozygous *Stgd3* mice was intermediate between these two extremes. Tg line A, the line with the greater restoration of lipid levels, showed the highest degree of recovery toward the loose leaflet structure of wt epidermis.

Further structural examination using electron microscopy detected interdigitation of stratum corneum corneocytes in homozygous *Stgd3* mice to an extent not seen in the wt or Tg/homozygous *Stgd3* mice (**Fig. 7B**). In addition, in homozygous *Stgd3* mice, transition cells were pres-

ent along the complete extent of the stratum granulosum/stratum corneum boundary, but were less frequent in the epidermis of wt and *Tg^A*/homozygous *Stgd3* mice (**Fig. 7B**). Prominent within the cytosol of homozygous *Stgd3* transition cells were entombed nuclear remnants and membrane-bound bodies, possibly including lamellar bodies (**Fig. 7B**). Such entombed bodies were also present in the cytosol of corneocytes in outer layers of the stratum corneum in both nonTg homozygous *Stgd3* and *Tg^C*/homozygous *Stgd3* mice (**Fig. 7C**). While such entombed bodies were rare in the corneocyte cytosol of *Tg^A*/homozygous *Stgd3* mice, lamellar granule-like, membrane-bound vesicles were observed in the interstices of corneocytes located a number of cellular layers above the stratum granulosum/stratum corneum interphase (**Fig. 7C**). The presence of these vesicles suggested that there was still some compromise of lamellar body processing, even though many morphological abnormalities of homozygous *Stgd3* epidermis had been rescued in Tg line A by transgene expression.

Transgene expression prevents neonatal lethality of homozygous *Stgd3* mice

Homozygous *Stgd3* mice have been shown to die within 1 h after birth with symptoms of defective skin barrier function (14). In contrast, the Tg/homozygous *Stgd3* mice derived from all three Tg lines remained viable. For the first few days of life, these mice were indistinguishable from their wt *Elovl4* littermates. However, after this initial period, the Tg/homozygous *Stgd3* mice failed to gain weight at the same rate as their wt *Elovl4* and heterozygous *Stgd3* littermates, with or without transgene expression. All Tg/homozygous *Stgd3* mice died during the first two weeks of life, with those from Tg line A, the line with the highest levels of restored skin lipids (**Fig. 2**), living the longest. These findings, combined with the biochemical, morphological, and functional analysis of the skin, led to the conclusion that the defective skin permeability barrier function is responsible for the death of neonatal homozygous *Stgd3* mice.

The presence of the same phenotype in Tg/homozygous *Stgd3* mice from all three Tg lines suggested a common origin for the shared pathology, most likely the suboptimal levels of Tg expression. To examine this possibility, we crossbred mice of Tg lines A and C (both on a *Stgd3/wt* background) to obtain *Tg^{A+C}* mice that carried both Tg insertion events on a homozygous *Stgd3* background. The *Tg^{A+C}*/homozygous *Stgd3* mice generated by this strategy lived longer than the Tg/homozygous *Stgd3* mice from either line A or C alone. These animals can live for more than one month, although at this age, they are still smaller than their wt or heterozygous *Stgd3* littermates (**Fig. 8**).

Tg^{A+C}/homozygous *Stgd3* mice express *Stgd3* mRNA but neither Tg nor *Elovl4* mRNA in the retina

Generation of viable *Tg^{A+C}*/homozygous *Stgd3* mice has created, for the first time, the opportunity to study how the mutation of both *Elovl4*-alleles affects *Elovl4*-expressing

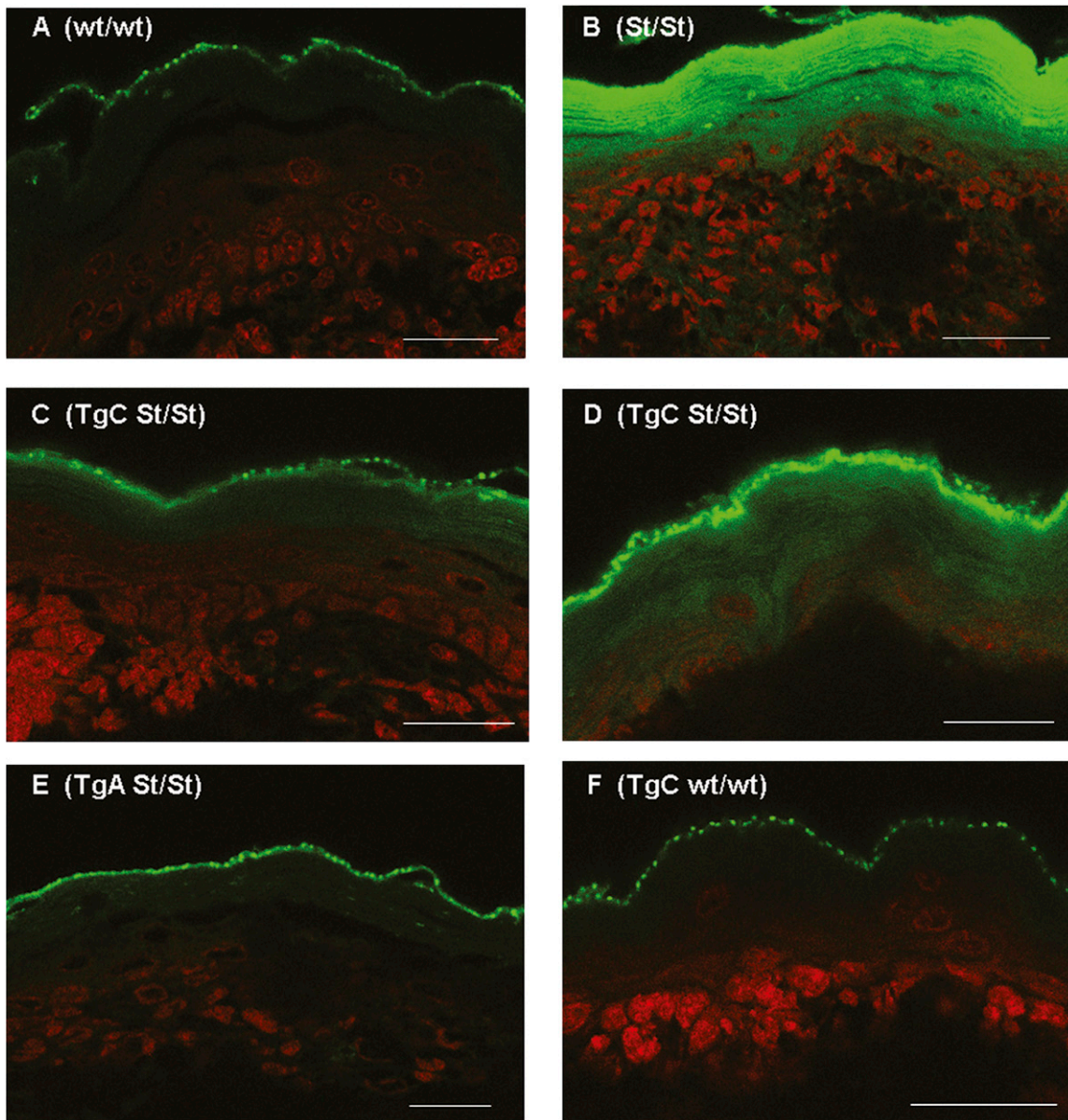


Fig. 6. Scanning confocal microscopy analysis showed Lucifer yellow staining (fluorescent signal assigned to the green channel) on the outer surface of the epidermal stratum corneum in euthanized neonatal mice of all studied genotypes. A: Staining of wt/wt epidermis. B: In homozygous *Stgd3* mice (*St/St*), the dye also penetrated and stained the full extent of the stratum corneum, with some penetration to lower epidermal strata. Compared with the homozygous *Stgd3* mice, staining of the interior of the stratum corneum was much weaker in both Tg/homozygous *Stgd3* mouse lines. In Tg line C (C and D: TgC *St/St*), the dye showed a variable level of penetration and more staining of interior stratum corneum than that observed in Tg line A (E: TgA *St/St*). F: Staining in a homozygous wt mouse carrying the Tg^C transgene (TgC wt/wt). All sections were counterstained with the nuclear TO-PRO-3 stain (signal in red). Scale bar = 30 μ m.

tissues of adult mice. The mature retina of wt mice contains high levels of both *Elovl4* mRNA and polyunsaturated C28-C36 fatty acids present as acyl residues in PCs (13, 14). In heterozygous *Stgd3* mice, the retina expresses equal amounts of *Stgd3* and *Elovl4* mRNAs, each present at 50% of the *Elovl4* mRNA level in wt mice. The reduced *Elovl4* mRNA level in heterozygous *Stgd3* mice is accompanied by a selective, approximately 50% reduction of retinal C28-C36 acyl PC amounts (13). This suggested that Tg^{A+C}/homozygous *Stgd3* mice should completely lack *Elovl4* mRNA and C28-C36 fatty acids in the retina and other nonsquamous epithelium-containing tissues.

To test this, we analyzed the retinas of three-week-old Tg^{A+C}/homozygous *Stgd3* mice for the presence of *Elovl4*, *Stgd3*, and Tg mRNA expression. Consistent with the use of the involucrin promoter to drive transgene expression, Tg mRNA was detected in the skin but not in the retinas of Tg^{A+C}/homozygous *Stgd3* mice (**Fig. 9**). In addition, as expected, these animals showed expression of *Stgd3* mRNA but not *Elovl4* mRNA in their retinas. Further retinal analysis showed that the absence of wt *Elovl4* and Tg mRNAs from the retinas of Tg^{A+C}/homozygous *Stgd3* mice was indeed associated with an expected complete lack of C28-C36 acyl PCs, the lipid products of the *Elovl4* pathway (W. Kedzierski, unpublished observations).

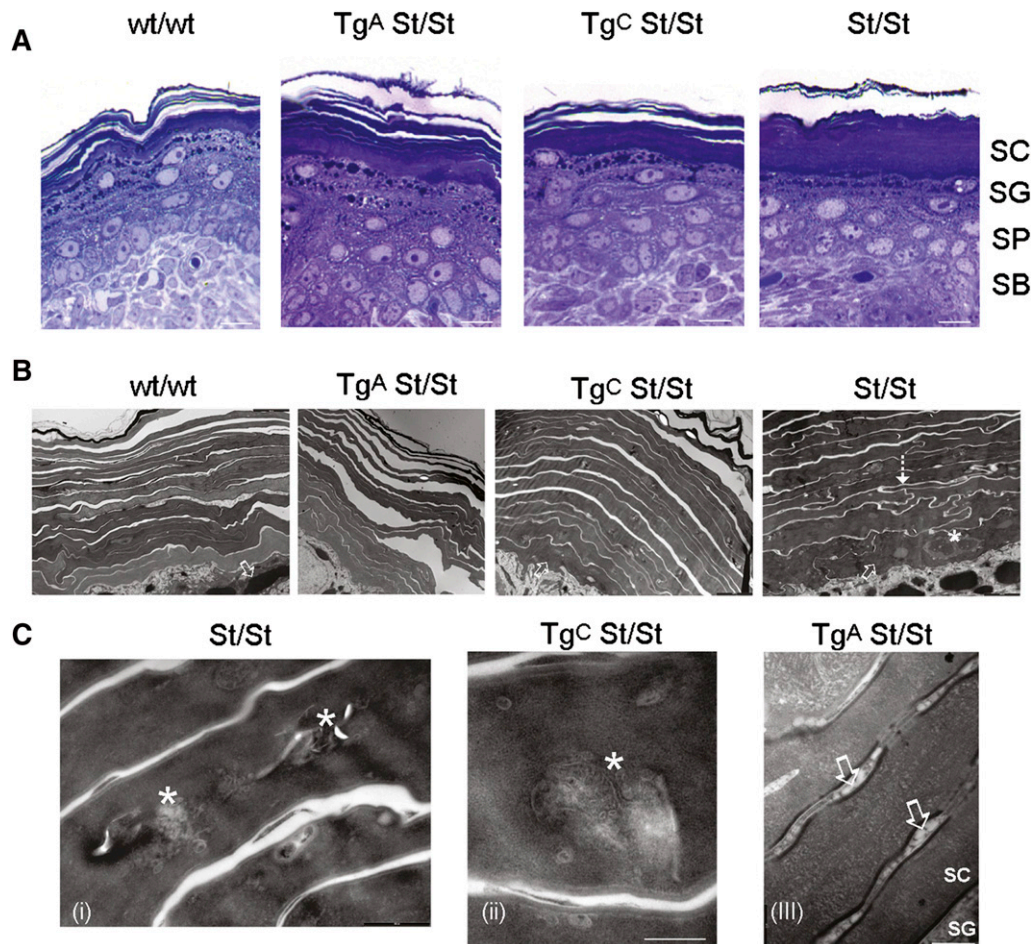


Fig. 7. Epidermal expression of the Elov14 transgene rescues structural changes in the skin of neonatal homozygous *Stgd3* mice. **A:** Light microscopic analysis shows a stack of loose layers present in the stratum corneum (SC) of wt mice (wt/wt) and in the outer stratum corneum in Tg/homozygous *Stgd3* mice of both lines (Tg^A St/St and Tg^C St/St). In the homozygous *Stgd3* mice (St/St), the stratum corneum forms a uniform, compact structure. No gross changes are observed in the stratum granulosum (SG), stratum spinosum (SP), or stratum basale (SB) among different mouse genotypes. Scale bar = 20 μ m. **B:** Electron microscopical analysis of stratum corneum in homozygous *Stgd3* mice detects extensive interdigitation of corneocytes (shown by dashed arrow), a feature not seen in wt or Tg homozygous *Stgd3* mice. In addition, the homozygous *Stgd3* mice contain transition cells along the complete extent of the boundary between the stratum granulosum and stratum corneum (shown by open arrows). These cells are also abundant in Tg^C mice but scarce in wt and Tg^A mice. In nonTg/homozygous *Stgd3* mice, the transition cells contain prominent undigested cellular contents, including nuclei (shown by asterisk). Scale bars = 2 μ m. **C:** Electron microscopical analysis detects cellular debris (shown by asterisks) still retained within corneocytes in outer layers of the stratum corneum in homozygous *Stgd3* mice (i) and, to a lesser degree, in Tg^C mice (ii). Although corneocyte cytosolic debris is less evident in Tg^A mice (iii), the lamellar body maturation is still delayed. It is evident by the membranous vesicles (shown by open arrows) present between corneocytes a number of layers above the stratum corneum/stratum granulosum junction. Scale bars (i) = 0.5, (ii) = 0.2, and (iii) = 0.2 μ m.

In conclusion, epidermal expression of the Elov14 transgene rescues the neonatal lethality of homozygous *Stgd3* mice. This approach generates a unique model system to study how the complete absence of C28-C36 fatty acid synthesis affects physiology of the retina and other nonskin tissues.

DISCUSSION

Mammals are known to express seven elongases that catalyze the addition of two carbon units to fatty acids containing 16 or more carbon atoms (5). Elov14 is the elongase

which has been shown to participate in synthesis of unusually long chain C28-C36 fatty acids (12–14, 17–19). Such fatty acids have been found in a few selected tissues, such as skin, brain, retina, meibomian gland, and testis (15). In these tissues, C28-C36 fatty acids occur as saturated, mono-unsaturated, or polyunsaturated acyl residues in unique, tissue-specific compound lipids. Studies in Elov14-mutant mice have already established that C28-C36 fatty acids are needed for the general well-being of mice (13, 14, 17–19). The present-day challenge is to determine the specific physiological roles these lipids play in Elov14-expressing tissues.

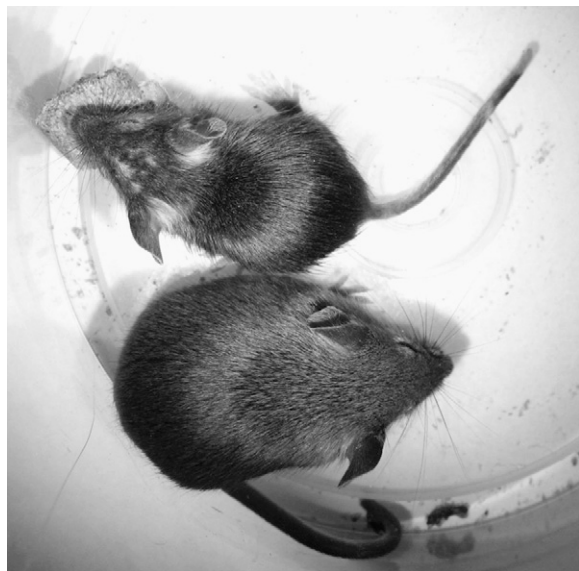


Fig. 8. One-month-old Tg^{A+C} /homozygous *Stgd3* male eating mouse chow (top of picture). The mouse is smaller than his *Tg* (not shown) and non*Tg*/heterozygous *Stgd3* male littermate (bottom of picture).

In this report, we demonstrate that the synthesis of C28-C36 fatty acids in the epidermis is absolutely required for mice to be viable beyond the neonatal period. Homozygous mutant mice that carry *Stgd3*, or other *Elovl4* mutations, die within a few h after birth (14, 17–19). A common feature in all these mice is the malformation of the stratum corneum, the outermost epidermal layer of the skin. Our current studies demonstrate that the neonatal lethality of homozygous *Stgd3* mice is prevented by the expression of the wt *Elovl4* transgene driven by the human involucrin promoter sequence (Fig. 1). This promoter directs transgene expression to stratified squamous epithelia which are present in the epidermal layer of the skin and in a few internal organs, such as the esophagus, forestomach, and tongue (20). This same involucrin promoter sequence has previously been used successfully to drive epidermal expression of different transgenes in several groups of transgenic mice (20, 26, 27).

Our previous studies in homozygous *Stgd3* mice established that these animals had a defective skin barrier function. However, whether the neonatal lethality in these mice was a sole consequence of absence of skin barrier function, or involved contributions from adverse responses to the absence of *Elovl4* lipids in other tissues was unknown. The demonstration that expression of the epidermal-targeted *Elovl4* transgene rescued both the skin barrier function and animal viability establishes that the neonatal lethality of homozygous *Stgd3* mice is indeed caused by the defect in the skin permeability barrier. In land-dwelling animals, the skin permeability barrier prevents dehydration and electrolyte disturbances. This barrier is formed late in embryogenesis by tight junctions within the stratum granulosum and by layers of corneocytes embedded in a matrix of extracellular lipid lamellae (28–31). The main components of the lipid matrix are

cholesterol, free fatty acids and ceramides. In mice, ceramide synthesis has been shown to be essential for the development and integrity of the epidermal permeability barrier (21, 32).

In our generated homozygous *Stgd3* mice, two abundant lipid groups of wt mouse epidermis were completely missing (Fig. 2). Previously, we identified one of these groups as acylceramides, lipids which contain residues of saturated and monounsaturated C28-C36 fatty acids (14). The second missing lipid group was identified in this study as (*O*-linoleoyl)-omega-hydroxy C32-C34 fatty acids. The existence of such lipids in human epidermis has previously been proposed based on studies involving lipid hydrolysis followed by component analysis (33). Although these lipids appear to be abundant, their function and origin in the epidermis remain unknown. It does seem, however, very likely that this lipid group shares some synthetic reactions with acylceramides, compound lipids which contain residues of (*O*-acyl)-omega-hydroxy C28-C36 fatty acids. This issue requires further studies since only key steps of the acylceramide biosynthetic pathway have been established (29, 31, 34). What our research does show, however, is that the biosynthetic pathways of both epidermal lipid groups depended on the *Elovl4*-mediated synthesis of C28-C36 fatty acids.

In addition to the restored synthesis of epidermal C28-C36 fatty acids, our studies demonstrate that *Elovl4* transgene expression corrects the key pathologic features of non*Tg* homozygous *Stgd3* mice: defective skin barrier function, abnormal epidermal morphology, and neonatal lethality. The *Tg*-mediated rescue of homozygous *Stgd3* skin pathology is not, however, complete. First, in all *Tg* mouse lines, the skin level of *Tg* mRNA is much lower than the amount of endogenous *Elovl4* mRNA (Fig. 1). This leads to reduced levels of epidermal C28-C36 acyl lipids in *Tg*/homozygous *Stgd3* mice compared with that in the wt mice (Fig. 2). Second, the Lucifer yellow dye penetration assay detects some flaws in the epidermal permeability barrier, especially in the low-expressing Tg^C mouse line (Fig. 6). Finally, microscopic analysis of neonatal skin in *Tg*/homozygous *Stgd3* mice shows a stratum corneum morphology which is intermediate between the loose basket weave-like structure seen in wt mice and the compact layer structure observed in homozygous *Stgd3* mice (Fig. 7). Corneocytes in the outer stratum corneum layers of *Tg*/homozygous *Stgd3* mice still retain cytosol-entombed, membrane-bounded bodies. In addition, lamellar body-like vesicles were noted in the interstices of corneocytes a number of layers above the stratum granulosum/stratum corneum boundary (Fig. 7). The presence of these bodies and vesicles, very rarely seen in wt stratum corneum layers, suggests that though certain morphological abnormalities have been rescued in *Tg* mouse lines, there is still some compromise of lamellar body processing. Future studies will be required to more fully characterize the nature of these morphological changes in *Tg* mouse lines differing in their levels of transgene expression. However, our current analyses of skin *Tg* mRNA, C28-C36 acyl lipids, morphology, and permeability barrier function all support the

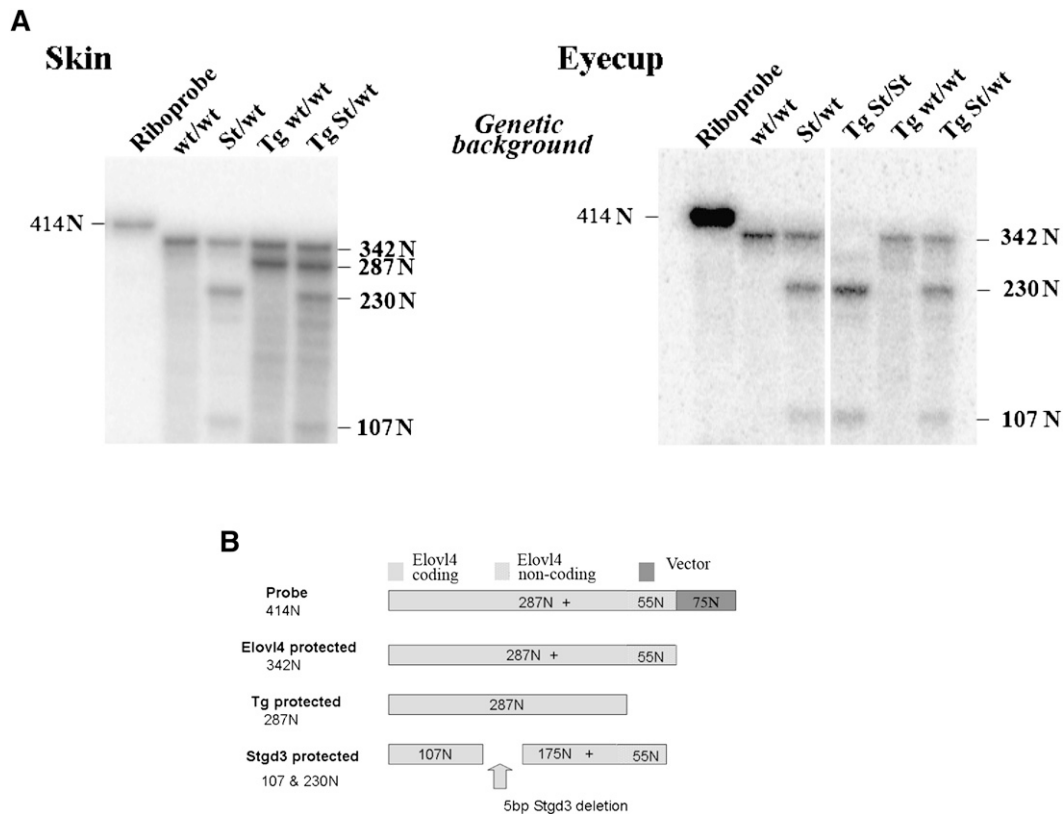


Fig. 9. Elov4 Tg mRNA is not expressed in the retina. Nuclease protection assay for wt Elov4, Stgd3, and Tg mRNAs. A: The skin of three-week-old Tg mice expresses Tg mRNA in addition to wt Elov4 mRNA and/or Stgd3 mRNA. The eyecups of three-week-old Tg^{A+C}/homozygous Stgd3 mice (Tg St/St) express Stgd3 mRNA but neither wt Elov4 mRNA nor Tg mRNA. In this assay, wt Elov4 mRNA protects a 342-N fragment of the 414-N riboprobe, Tg mRNA protects a 287-N fragment, and Stgd3 mRNA protects two fragments of 230 and 107 Ns, as shown in schematic form in B.

conclusion that the epidermal expression of the Elov4 transgene is responsible for the rescue of the neonatal lethality of homozygous Stgd3 mice. Further proof is provided by the observation of the longer survival of Tg^{A+C}/homozygous Stgd3 mice relative to the mono-Tg, either Tg^A or Tg^C, mice.


In conclusion, our approach generates viable Tg/homozygous Stgd3 mice lacking C28-C36 fatty acid synthesis in tissues which do not express the Elov4 transgene. Of particular interest in this regard is the potential use of these mice in studies to define the function of C28-C36 acyl PCs in mature retinal physiology. Prior to such studies it is necessary, however, to establish absence of Elov4 transgene expression in the retina.

In Tg^{A+C}/homozygous Stgd3 mice, mature retinas express Stgd3 mRNA but neither wt Elov4 mRNA nor Tg mRNA (Fig. 9). In addition, our recent studies show that retinal C28-C36 acyl PCs are totally missing in these mice, which is consistent with the lack of wt Elov4 mRNA expression (W. Kedzierski, unpublished observations). The absence of C28-C36 acyl PCs also suggests no retinal uptake of any C28-C36 fatty acids potentially secreted to the circulation from transgene-expressing tissues. Therefore, the generated Tg^{A+C}/homozygous Stgd3 mice can now be used to determine the biological functions of C28-C36

fatty acids in the retina, as well as in many other Elov4-expressing tissues.

Tg^{A+C}/homozygous Stgd3 mice are smaller compared with their wt or heterozygous Stgd3 littermates, either Tg or nonTg. In addition to the still compromised skin barrier function, it is also possible that some other physiological changes induced by the absence of endogenous C28-C36 fatty acid synthesis may contribute to the observed pathology. At 3-4 weeks of age, these animals are smaller by about 40%. Also at this age, smaller and weaker mice quite often die. However, the majority of mutant mice survive this critical period of transition from mother's milk to a solid diet. Surviving mice continue to gain weight, especially when kept on a high-fat diet. The Tg^{A+C}/homozygous Stgd3 mice can live for at least 2-3 months, an age at which they have mature retinas and other organs suitable for research.

In the future, our studies in Tg/homozygous Stgd3 mice can be supplemented by studies in mice with Cre-mediated, tissue-specific Elov4 gene knockouts. Generation of the latter mice has already been undertaken by the High Throughput Gene Targeting Group at the European Conditional Mouse Mutagenesis Program (<http://www.eucomm.org/links/>). We feel strongly that studies using mice from both model systems will complement each other by creating slightly different research opportunities which will

successfully *a*) identify the physiological functions of C28-C36 acyl lipids in Elov14-expressing tissues, *b*) determine the pathogenic mechanism of Stargardt-3 disease, and *c*) help in the design of potential treatments for this human macular pathology. 

The authors thank Dr. Ingo Haase (University of Cologne, Cologne, Germany) for expert advice regarding use of the involucrin promoter for transgene construction. The authors also thank Dr. Soosan Ghazizadeh (State University of New York, Stony Brook, NY) who kindly sent us the involucrin promoter-containing plasmid pH3700-pL2, a plasmid originally generated by Dr. Lorne B. Taichman (State University of New York, Stony Brook, NY).

REFERENCES

- Zhang, K., M. Kniazeva, M. Han, W. Li, Z. Yu, Z. Yang, Y. Li, M. L. Metzker, R. Allikmets, D. J. Zack, et al. 2001. A 5-bp deletion in ELOVL4 is associated with two related forms of autosomal dominant macular dystrophy. *Nat. Genet.* **27**: 89–93.
- Edwards, A. O., L. A. Donoso, and R. Ritter 3rd. 2001. A novel gene for autosomal dominant Stargardt-like macular dystrophy with homology to the SUR4 protein family. *Invest. Ophthalmol. Vis. Sci.* **42**: 2652–2663.
- Bernstein, P. S., J. Tammur, N. Singh, A. Hutchinson, M. Dixon, C. M. Pappas, N. A. Zabriskie, K. Zhang, K. Petrukhin, M. Leppert, et al. 2001. Diverse macular dystrophy phenotype caused by a novel complex mutation in the ELOVL4 gene. *Invest. Ophthalmol. Vis. Sci.* **42**: 3331–3336.
- Maugeri, A., F. Meire, C. B. Hoyng, C. Vink, N. Van Regemorter, G. Karan, Z. Yang, F. P. Cremers, and K. Zhang. 2004. A novel mutation in the ELOVL4 gene causes autosomal dominant Stargardt-like macular dystrophy. *Invest. Ophthalmol. Vis. Sci.* **45**: 4263–4267.
- Jakobsson, A., R. Westerberg, and A. Jacobsson. 2006. Fatty acid elongases in mammals: their regulation and roles in metabolism. *Prog. Lipid Res.* **45**: 237–249.
- Ambasudhan, R., X. Wang, M. M. Jablonski, D. A. Thompson, P. S. Lagali, P. W. Wong, P. A. Sieving, and R. Ayyagari. 2004. Atrophic macular degeneration mutations in ELOVL4 result in the intracellular misrouting of the protein. *Genomics.* **83**: 615–625.
- Karan, G., Z. Yang, and K. Zhang. 2004. Expression of wild type and mutant ELOVL4 in cell culture: subcellular localization and cell viability. *Mol. Vis.* **10**: 248–253.
- Grayson, C., and R. S. Molday. 2005. Dominant negative mechanism underlies autosomal dominant Stargardt-like macular dystrophy linked to mutations in ELOVL4. *J. Biol. Chem.* **280**: 32521–32530.
- Vasireddy, V., C. Vijayarathy, J. Huang, X. F. Wang, M. M. Jablonski, H. R. Petty, A. A. Sieving, and R. Ayyagari. 2005. Stargardt-like macular dystrophy protein ELOVL4 exerts a dominant negative effect by recruiting wild-type protein into aggresomes. *Mol. Vis.* **11**: 665–676.
- Karan, G., Z. Yang, K. Howes, Y. Zhao, Y. Chen, D. J. Cameron, Y. Lin, E. Pearson, and K. Zhang. 2005. Loss of ER retention and sequestration of the wild-type ELOVL4 by Stargardt disease dominant negative mutants. *Mol. Vis.* **11**: 657–664.
- Wang, Y., D. Botolin, B. Christian, J. Busik, J. Xu, and D. B. Jump. 2005. Tissue-specific, nutritional, and developmental regulation of rat fatty acid elongases. *J. Lipid Res.* **46**: 706–715.
- Agbaga, M. P., R. S. Brush, M. N. Mandal, K. Henry, M. H. Elliott, and R. E. Anderson. 2008. Role of Stargardt-3 macular dystrophy protein (ELOVL4) in the biosynthesis of very long chain fatty acids. *Proc. Natl. Acad. Sci. USA.* **105**: 12843–12848.
- McMahon, A., S. N. Jackson, A. S. Woods, and W. Kedzierski. 2007. A Stargardt disease-3 mutation in the mouse Elov4 gene causes retinal deficiency of C32-C36 acyl phosphatidylcholines. *FEBS Lett.* **581**: 5459–5463.
- McMahon, A., I. A. Butovich, N. L. Mata, M. Klein, R. Ritter 3rd, J. Richardson, D. G. Birch, A. O. Edwards, and W. Kedzierski. 2007. Retinal pathology and skin barrier defect in mice carrying a Stargardt disease-3 mutation in elongase of very long chain fatty acids-4. *Mol. Vis.* **13**: 258–272.
- McMahon, A., and W. Kedzierski. 2010. Polyunsaturated very-long-chain C28-C36 fatty acids and retinal physiology. *Br. J. Ophthalmol.* **94**: 1127–1132.
- Mandal, M. N., R. Ambasudhan, P. W. Wong, P. J. Gage, P. A. Sieving, and R. Ayyagari. 2004. Characterization of mouse orthologue of ELOVL4: genomic organization and spatial and temporal expression. *Genomics.* **83**: 626–635.
- Cameron, D. J., Z. Tong, Z. Yang, J. Kaminoh, S. Kamiyah, H. Chen, J. Zeng, Y. Chen, L. Luo, and K. Zhang. 2007. Essential role of Elov4 in very long chain fatty acid synthesis, skin permeability barrier function, and neonatal survival. *Int. J. Biol. Sci.* **3**: 111–119.
- Li, W., R. Sandhoff, M. Kono, P. Zerfas, V. Hoffmann, B. C. Ding, R. L. Proia, and C. X. Deng. 2007. Depletion of ceramides with very long chain fatty acids causes defective skin permeability barrier function, and neonatal lethality in ELOVL4 deficient mice. *Int. J. Biol. Sci.* **3**: 120–128.
- Vasireddy, V., Y. Uchida, N. Salem, Jr., S. Y. Kim, M. N. Mandal, G. B. Reddy, R. Bodepudi, N. L. Alderson, J. C. Brown, H. Hama, et al. 2007. Loss of functional ELOVL4 depletes very long-chain fatty acids (> or =C28) and the unique omega-O-acylceramides in skin leading to neonatal death. *Hum. Mol. Genet.* **16**: 471–482.
- Carroll, J. M., K. M. Albers, J. A. Garlick, R. Harrington, and L. B. Taichman. 1993. Tissue- and stratum-specific expression of the human involucrin promoter in transgenic mice. *Proc. Natl. Acad. Sci. USA.* **90**: 10270–10274.
- Doering, T., H. Brade, and K. Sandhoff. 2002. Sphingolipid metabolism during epidermal barrier development in mice. *J. Lipid Res.* **43**: 1727–1733.
- Butovich, I. A., J. Wojtowicz, and M. Molai. 2009. Human tear film and meibum. I. Very long chain wax esters and (O-acyl)-omega-hydroxy fatty acids of meibum. *J. Lipid Res.* **50**: 2471–2485.
- Mirza, R., S. Hayasaka, Y. Takagishi, F. Kambe, S. Ohmori, K. Maki, M. Yamamoto, K. Murakami, T. Kaji, D. Zadworny, et al. 2006. DHCR24 gene knockout mice demonstrate lethal dermopathy with differentiation and maturation defects in the epidermis. *J. Invest. Dermatol.* **126**: 638–647.
- Suga, Y., M. Jarnik, P. S. Attar, M. A. Longley, D. Bundman, A. C. Steven, P. J. Koch, and D. R. Roop. 2000. Transgenic mice expressing a mutant form of loricrin reveal the molecular basis of the skin diseases, Vohwinkel syndrome and progressive symmetric erythrokeratoderma. *J. Cell Biol.* **151**: 401–412.
- Mauldin, E. A., K. M. Credille, R. W. Dunstan, and M. L. Casal. 2008. The clinical and morphologic features of nonepidermolytic ichthyosis in the golden retriever. *Vet. Pathol.* **45**: 174–180.
- Jaubert, J., S. Patel, J. Cheng, and J. A. Segre. 2004. Tetracycline-regulated transactivators driven by the involucrin promoter to achieve epidermal conditional gene expression. *J. Invest. Dermatol.* **123**: 313–318.
- Brennan, D., Y. Hu, S. Joubert, Y. W. Choi, D. Whitaker-Menezes, T. O'Brien, J. Uitto, U. Rodeck, and M. G. Mahoney. 2007. Suprabasal Dsg2 expression in transgenic mouse skin confers a hyperproliferative and apoptosis-resistant phenotype to keratinocytes. *J. Cell Sci.* **120**: 758–771.
- Feingold, K. R. 2007. The importance of lipids in cutaneous function. *J. Lipid Res.* **48**: 2529–2530.
- Uchida, Y., and W. M. Holleran. 2008. Omega-O-acylceramide, a lipid essential for mammalian survival. *J. Dermatol. Sci.* **51**: 77–87.
- Choi, M. J., and H. I. Maibach. 2005. Role of ceramides in barrier function of healthy and diseased skin. *Am. J. Clin. Dermatol.* **6**: 215–223.
- Sandhoff, R. 2010. Very long chain sphingolipids: tissue expression, function and synthesis. *FEBS Lett.* **584**: 1907–1913.
- Jennemann, R., R. Sandhoff, L. Langbein, S. Kaden, U. Rothermel, H. Gallala, K. Sandhoff, H. Wiegandt, and H. J. Grone. 2007. Integrity and barrier function of the epidermis critically depend on glucosylceramide synthesis. *J. Biol. Chem.* **282**: 3083–3094.
- Wertz, P. W., and D. T. Downing. 1988. Hydroxyacid derivatives in human epidermis. *Lipids.* **23**: 415–418.
- Mizutani, Y., S. Mitsutake, K. Tsuji, A. Kihara, and Y. Igarashi. 2009. Ceramide biosynthesis in keratinocyte and its role in skin function. *Biochimie.* **91**: 784–790.